

# H $\alpha$ STAR FORMATION RATES FOR A SAMPLE OF STAR-FORMING GALAXIES FROM SDSS (DR1)

I. Y. Izotova<sup>1</sup>, S. L. Parnovsky<sup>1</sup>, Y. I. Izotov<sup>2</sup>

<sup>1</sup>*Astronomical Observatory, National Taras Shevchenko University of Kyiv  
3 Observatorna Str., 04053 Kyiv, Ukraine  
e-mail: izotova@observ.univ.kiev.ua*

<sup>2</sup>*Main Astronomical Observatory, NAS of Ukraine  
27 Akademika Zabolotnoho Str., 03680 Kyiv, Ukraine*

---

A study of current star formation rates (SFRs) derived from H $\alpha$  emission of ionized hydrogen for 1305 star-forming galaxies from the Sloan Digital Sky Survey (Data Release 1) is carried out. Current SFRs are derived from the H $\alpha$  flux corrected for interstellar extinction and aperture. For a subsample of 45 galaxies the current SFRs are derived using simultaneously three parameters: the galaxy luminosity in the far infrared range (IRAS data), the monochromatic radio continuum luminosity at 1.4 GHz (NVSS data), and the H $\alpha$  emission of ionized hydrogen (SDSS DR1 data). The results obtained are discussed and compared with the similar ones for the Markarian galaxies.

---

## INTRODUCTION

Star formation in a galaxy is characterized by two main parameters: the initial mass function (IMF) and the total star formation rate (SFR). The emission in the far infrared range (FIR), the radio continuum emission at 1.4 GHz, and the H $\alpha$  emission of ionized hydrogen are the main indicators of star-forming processes in the galaxy. A star formation rate averaged over a timescale of  $10^7$ – $10^8$  yr is defined as a current SFR. Studies of current SFRs have been carried out in [4–6, 9–13]. In this paper we present a study of current SFRs for a homogeneous sample of 1305 galaxies with active star formation processes using data from the Data Release 1 of the Sloan Digital Sky Survey (SDSS DR1). Throughout the paper we assume the Hubble constant to be  $H_0 = 75 \text{ km s}^{-1} \text{ Mpc}^{-1}$ .

## THE SAMPLE

The Sloan Digital Sky Survey is a photometric and spectroscopic survey which was carried out with a dedicated 2.5-m telescope at the Apache Point Observatory in New Mexico and was aimed to get a digital map of the North Galactic Cap in the area of  $10\,000 \text{ deg}^2$ . The SDSS Data Release 1 [1] has been released in 2003. SDSS DR1 covers the sky region of  $2099 \text{ deg}^2$  with imaging data in five bands  $u, g, r, i, z$  (at wavelengths 3551 Å, 4886 Å, 6166 Å, 7480 Å, and 8932 Å, respectively), more than 180 000 spectra of galaxies, quasars, and stars selected over  $1360 \text{ deg}^2$  of this area. The imaging data stretch to a depth of about  $r \sim 22.6$ , the spectra cover the wavelength interval 3800–9200 Å with a resolution of 1800–2100.

For SFRs study we use a sample of 1338 emission-line galaxies which were extracted from SDSS DR1 after an examination of all  $\sim 180\,000$  spectra [8]. The galaxies from this sample have an emission feature at the wavelength of the [O III] 4363. The presence of this emission line allows one to provide the direct model-independent determination of the electron temperature and abundance. The H $\alpha$  fluxes have been corrected for interstellar extinction using the observed hydrogen Balmer emission-line fluxes [8] as well as for aperture effect. The latter procedure is done using the ratio of the fluxes corresponding to the total galaxy magnitude  $m$  and the magnitude  $m(3'')$  “through the fiber” in the  $r$  band (for redshifts  $z < 0.04$ ) and in the  $i$  band (for redshifts  $z \geq 0.04$ ) ( $N = 1305$ ). The fiber magnitude is taken from a photometric measurement in a  $3''$  fiber aperture. The aperture correction factor can be expressed as  $A = 10^{-0.4[m_{r,i} - m_{r,i}(3'')]}$ .

This galaxy sample was cross-identified with the NVSS sources [3] having the 1.4 GHz radio continuum radiation and the IRAS/IRASF catalogue sources [7]. For this purpose, we combine NVSS, IRAS/IRASF, NED<sup>1</sup> data and SDSS images with due regard for size of radio sources. We have revealed that 100 galaxies from our sample are NVSS sources, 102 galaxies are IRAS/IRASF sources, and 45 emission-line galaxies are

---

© I. Y. Izotova, S. L. Parnovsky, Y. I. Izotov, 2004

<sup>1</sup>The NASA/IPAC Extragalactic Database operated by the Jet Propulsion Laboratory, California Institute of Technology.

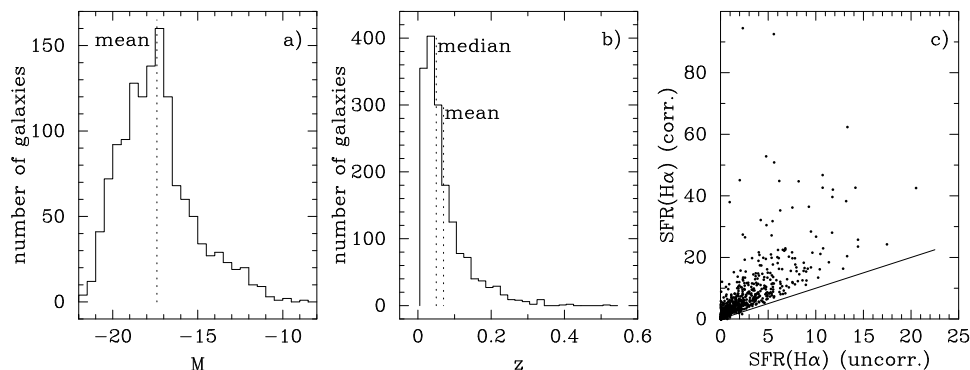


Figure 1. (a) Distribution of the galaxy absolute magnitudes. (b) Redshift distribution for a sample of galaxies. (c) Comparison of uncorrected values of SFR( $H\alpha$ ) derived from the luminosity in the  $H\alpha$  line of ionized hydrogen with the corrected ones

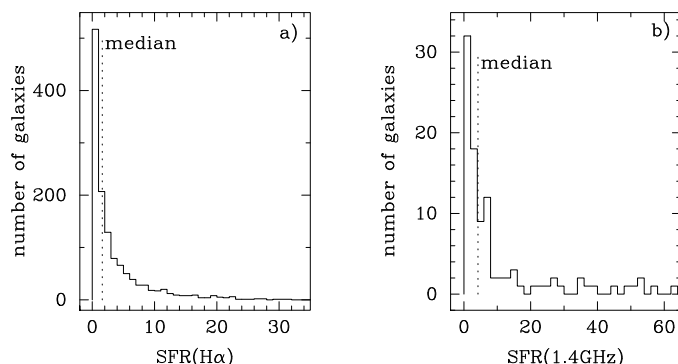


Figure 2. (a) Distribution of SFRs derived from the luminosity in the  $H\alpha$  line of ionized hydrogen. (b) Distribution of SFRs derived from the radio continuum emission at 1.4 GHz

the sources found both in NVSS and IRAS/IRASF. The distributions of the galaxy absolute magnitudes  $M$  and redshifts  $z$  for the whole sample of 1338 galaxies are shown in Figs. 1a–1b with a median  $M = -17.6$  and a median  $z = 0.046$ .

## STAR FORMATION RATES

The current star formation rate can be obtained from the luminosity of a H II region in the  $H\alpha$  emission line or in the radio continuum. For deriving of the SFRs, the free-free radiation in the radio continuum is preferable in general because of negligible extinction in the radio range, but this method is limited by a lower sensitivity and confusion with non-thermal sources. Both optical and radio methods suffer from absorption of Ly- $c$  photons by dust that re-radiates energy in the far infrared range. Following to the approach in [4, 6], we assume the Salpeter IMF with a slope coefficient  $\alpha = 2.35$ , low- and high- star mass cut-offs of  $0.1 M_{\odot}$  and  $100 M_{\odot}$ , respectively. Then, the current SFR (averaged over star lifetime of  $\sim 3 \cdot 10^6$  yr) is defined as

$$\text{SFR}(H\alpha) = 7.07 \cdot 10^{-42} L(H\alpha), \quad (1)$$

where  $L(H\alpha)$  is the galaxy luminosity in the  $H\alpha$  emission line of ionized hydrogen corrected for interstellar extinction and aperture effect, it is in  $\text{erg s}^{-1}$ ;  $\text{SFR}(H\alpha)$  is in  $M_{\odot} \text{ yr}^{-1}$ .

It is assumed in Eq. (1) that 1/3 of the Ly- $c$  flux is lost due to dust absorption or escapes from the galaxy. The coefficient in the relation between  $\text{SFR}(H\alpha)$  and  $L(H\alpha)$  in Eq. (1) depends on the adopted IMF and metallicity [13].

The luminosities  $L(H\alpha)$  corrected for interstellar extinction and aperture effect in individual galaxies are a few times larger than the uncorrected ones (Fig. 1c). The individual SFRs( $H\alpha$ ) for the total sample vary in a wide range of  $10^{-3} \div 439.6 M_{\odot} \text{ yr}^{-1}$  with a median  $\text{SFR}(H\alpha) = 1.6 M_{\odot} \text{ yr}^{-1}$  (Fig. 2a).

To obtain  $\text{SFR}(1.4\text{GHz})$ , we assume that the radiation at 1.4 GHz is thermal [9]. In fact, a substantial part of this radiation can be a non-thermal one produced by young supernovae or old supernovae remnants.

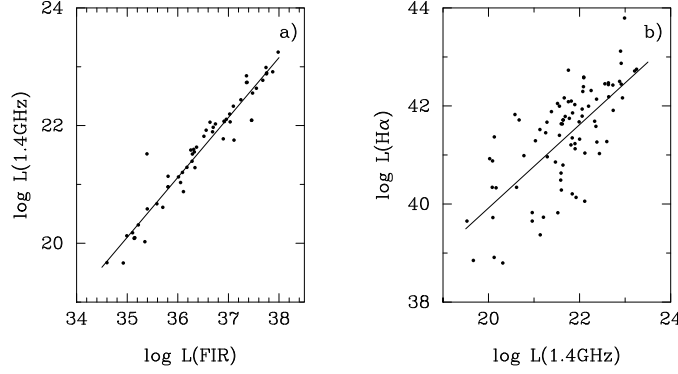


Figure 3. (a) The luminosity  $\log L(\text{FIR})$  dependence on the luminosity  $\log L(1.4\text{GHz})$ . (b) The luminosity  $\log L(1.4\text{GHz})$  dependence on the luminosity  $\log L(\text{H}\alpha)$

The fraction of thermal radiation is shown to be about 10% of the total flux for normal galaxies [2]. Taking into account this fraction, we obtain in accordance with [9]:

$$\text{SFR}(1.4\text{ GHz}) = 2.5 \cdot 10^6 \alpha L(1.4\text{ GHz}) / L_{\odot} M_{\odot}\text{yr}^{-1}, \quad (2)$$

where  $\alpha = 0.1$ ,  $L(1.4\text{GHz})/L_{\odot} = 3.07 \cdot 10^{-7} D^2 f_{1.4}$  is the galaxy radio continuum luminosity,  $D$  is the distance in Mpc,  $f_{1.4}$  is the flux density in Jy.

We can derive the current SFR in the galaxy from its far infrared luminosity following to [12]:

$$\text{SFR}(\text{FIR}) = 6.5 \cdot 10^{-10} L_{\text{FIR}} / L_{\odot} M_{\odot}\text{yr}^{-1}. \quad (3)$$

Eq. (3) is obtained assuming that  $UV$  radiation of the massive OB-stars is completely absorbed by dust and re-emitted in the far-infrared range. The far infrared  $60\ \mu\text{m}$  and  $100\ \mu\text{m}$  emission flux densities from IRAS/IRASF catalogues are used to derive the total galaxy FIR luminosity

$$L_{\text{FIR}} / L_{\odot} = 3.89 \cdot 10^5 [2.58 S_{60}(\text{Jy}) + S_{100}(\text{Jy})] D^2. \quad (4)$$

Note that Eqs. (1) and (3) are obtained assuming the same IMF and masses, and star lifetime of  $\sim 3 \cdot 10^6$  yr.

We derive the current  $\text{SFR}(\text{FIR})$  and  $\text{SFR}(1.4\text{GHz})$  for those galaxies from our sample of emission-line galaxies from SDSS which match with sources from the IRAS/IRASF catalogues and NVSS data. Similar to  $\text{SFR}(\text{H}\alpha)$ , the individual values of the  $\text{SFR}(\text{FIR})$  and  $\text{SFR}(1.4\text{GHz})$  vary in the large intervals:  $\text{SFR}(\text{FIR}) = 0.03 \div 162.1 M_{\odot}\text{yr}^{-1}$  ( $N = 102$ ) with a median  $\text{SFR}(\text{FIR}) = 2.8 M_{\odot}\text{yr}^{-1}$  and  $\text{SFR}(1.4\text{GHz}) = 0.02 \div 114.8 M_{\odot}\text{yr}^{-1}$  ( $N = 100$ ) with a median  $\text{SFR}(1.4\text{GHz}) = 4.2 M_{\odot}\text{yr}^{-1}$  (Fig. 2b). For comparison, HII galaxies from the First Byurakan Survey (FBS) detected by IRAS have a median  $\text{SFR}(\text{FIR})_{\text{FBS}} = 16.1 M_{\odot}\text{yr}^{-1}$  ( $N = 442$ ), a median  $\text{SFR}(1.4\text{GHz})_{\text{FBS}} = 4.9 M_{\odot}\text{yr}^{-1}$  ( $N = 435$ ), in accordance with [10], if one takes into account the fraction of thermal radiation for normal galaxies from [2]. Thus on the face of it, the SDSS emission-line galaxies are characterized by lower star formation rates derived from FIR luminosities in comparison with the Markarian ones. This is mainly caused by the fact that Markarian galaxies are brighter as compared with the SDSS emission-line ones and, hence, they are more metal-rich and contain more dust.

The dependence of the 1.4 GHz luminosity on the FIR luminosity in log scale (Fig. 3a) for a SDSS galaxies sample has the same tight linear correlation (with coefficient  $R = 0.92$ , slope of 1.02) as it was revealed earlier for Markarian galaxies. Tight correlation implies the common origin of the FIR radiation and radio continuum emission in the star-forming regions. However, contrary to expectations, no tight correlation was obtained between the  $\text{H}\alpha$  luminosities and 1.4 GHz luminosities (Fig. 3b). The possible reason for such differences might be due to the inhomogeneous distribution of dust in star-forming regions and uncertainties in the interstellar extinction.  $\text{H}\alpha$  luminosity is most subject to this effect while the 1.4 GHz and FIR luminosities are not.

Some characteristics such as redshift  $z$ , absolute magnitude  $M(r)$  in the  $r$  band as well as  $\text{SFR}(\text{H}\alpha)$ ,  $\text{SFR}(\text{FIR})$ , and  $\text{SFR}(1.4\text{GHz})$  derived from Eqs. (1)–(3) for emission-line galaxies from SDSS and HII Markarian galaxies detected by IRAS are shown in Table 1. In the paper by Hopkins *et al.* [5], the current star formation rates based on the  $\text{H}\alpha$ , FIR, and 1.4 GHz luminosities are derived using other relations between the SFRs and respective luminosities. Adopting Eqs. (1)–(2), (7)–(8) from [5]

we obtain for our sample:  $\text{SFR}(\text{FIR})_H = 0.07 \div 72.6 M_{\odot}\text{yr}^{-1}$  with a median  $\text{SFR}(\text{FIR})_H = 1.4 M_{\odot}\text{yr}^{-1}$ ;  $\text{SFR}(1.4\text{GHz})_H = 0.07 \div 98 M_{\odot}\text{yr}^{-1}$  with a median  $\text{SFR}(1.4\text{GHz})_H = 2.4 M_{\odot}\text{yr}^{-1}$ . Thus, calibrations used in the present paper do not differ significantly from those used by Hopkins *et al.* [5].

Table 1. Comparison of SFRs and other characteristics for the SDSS emission-line galaxies and Markarian H II galaxies

Parameter	SDSS emission-line galaxies		Markarian H II galaxies (with FIR)	
	Interval	Median	Interval	Median
$z$	$0.000142 \div 0.538$	0.046	$0.001 \div 0.163$	0.022
$M(r)$	$-8.7 \div -21.8$	-17.60	$-15.7 \div -22.2$	-19.7
$\text{SFR}(\text{H}\alpha), M_{\odot}\text{yr}^{-1}$	$10^{-3} \div 439.6$	1.6	—	—
$\text{SFR}(\text{FIR}), M_{\odot}\text{yr}^{-1}$	$0.03 \div 162.1$	2.8	$0.2 \div 344.3$	16.1
$\text{SFR}(1.4\text{GHz}), M_{\odot}\text{yr}^{-1}$	$0.02 \div 114.8$	4.2	$0.3 \div 3.2 \cdot 10^3$	4.9

## CONCLUSION

For a sample of the SDSS emission-line galaxies we derived the current star formation rates  $\text{SFR}(\text{H}\alpha)$ ,  $\text{SFR}(\text{FIR})$ ,  $\text{SFR}(1.4\text{GHz})$  based on the following indicators: the  $\text{H}\alpha$  emission of ionized hydrogen, galaxy emission in the far infrared range ( $60 \mu\text{m}$  and  $100 \mu\text{m}$ ), and radio continuum radiation at 1.4 GHz.

SDSS emission-line galaxies are shown to be characterized by lower star formation rates derived from FIR luminosities in comparison with the Markarian galaxies. This difference is mainly because of the lower luminosities of the SDSS galaxies. Hence, SDSS galaxies are more metal-poor and contain less dust which is responsible for FIR emission but not for the  $\text{H}\alpha$  or 1.4 GHz emission. The fact that the SFRs in SDSS galaxies derived from the  $\text{H}\alpha$  luminosity are lower than  $\text{SFRs}(\text{FIR})$ , and  $\text{SFRs}(1.4\text{GHz})$  implies the inhomogeneous distribution of dust in star-forming regions. Therefore, the large fraction of  $\text{H}\alpha$  emission is probably hidden in the densest central parts of star-forming regions due to higher interstellar extinction.

- [1] Abazajian K., Adelman-McCarthy J. K., Agueros M. A., *et al.* The First Data Release of the Sloan Digital Sky Survey // *Astron. J.*–2003.–**126**, N 4.–P. 2081–2086.
- [2] Condon J. J. Radio emission from normal galaxies // *Annu. Rev. Astron. and Astrophys.*–1995.–**30**.–P. 575–611.
- [3] Condon J. J., Cotton W. D., Greisen E. W., *et al.* The NRAO VLA Sky Survey // *Astron. J.*–1998.–**115**, N 5.–P. 1693–1716.
- [4] Gallagher III J. S., Hunter D. A., Tutukov A. V. Star formation histories of irregular galaxies // *Astrophys. J.*–1984.–**284**, N 2.–P. 544–556.
- [5] Hopkins A. M., Miller C. J., Nichol R. C., *et al.* Star Formation Rate Indicators in the Sloan Digital Sky Survey // *Astrophys. J.*–2003.–**599**, N 2.–P. 971–991.
- [6] Hunter D. A., Gallagher III J. S. Stellar populations and star formation in irregular galaxies // *Publ. Astron. Soc. Pacif.*–1986.–**98**, N 1.–P. 5–28.
- [7] IRAS catalog and Atlases: Explanatory Supplement / Eds C. A. Beichman, G. Neugebauer, H. J. Habing, P. E. Clegg, T. J. Chester, 2004.–80 p.
- [8] Izotov Y. I., Stasińska G., Guseva N. G., Thuan T. X. Abundance patterns in the low-metallicity emission-line galaxies from the Early Data Release of the Sloan Digital Sky Survey // *Astron. and Astrophys.*–2004.–**415**, N 1.–P. 87–94.
- [9] Izotova I. Y., Izotov Y. I. Star formation rate in blue compact galaxies from the Second Byurakan Survey // *Kinematics and Physics of Celestial Bodies.*–1999.–**15**, N 3.–P. 195–205.
- [10] Izotova I. Y., Parnovsky S. L. Star formation rate in Markarian galaxies // *Kinematics and Physics of Celestial Bodies. Suppl. Ser.*–2000.–N 3.–P. 99–100.
- [11] Izotova I. Y., Parnovsky S. L., Izotov Y. I. Star Formation Rate in Starburst Galaxies // *New Astron. Rev.*–2000.–**44**, N 3.–P. 283–285.
- [12] Thronson H. A., Telesco C. H. Star formation in active dwarf galaxies // *Astrophys. J.*–1986.–**311**, N 1.–P. 98–112.
- [13] Zasov A. V. The efficiency of star formation in spiral galaxies // *Astron. Lett.*–1995.–**21**, N 5.–P. 652–662.